

## XeCl Excimer Laser Annealing Used to Fabricate Poly-Si TFT's

Toshiyuki SAMESHIMA, Masaki HARA and Setsuo USUI

Sony Research Center, 174 Fujitsuka-cho, Hodogaya-ku, Yokohama 240

(Received June 28, 1989; revised manuscript received July 27, 1989;  
accepted for publication August 19, 1989)

Polycrystalline silicon thin-film transistors (poly-Si TFT's) with a high carrier mobility were fabricated at low processing temperatures of 150 and 250°C. A hydrogenated amorphous silicon (a-Si:H) film was successfully crystallized at room temperature by multistep irradiation of XeCl-308 nm excimer laser pulses without explosive evaporation of hydrogen. The poly-Si TFT's fabricated by the 250°C process had a carrier mobility of 54 cm<sup>2</sup>/V·s and a low potential barrier height at a grain boundary of 0.01 eV.

**KEYWORDS:** hydrogenated amorphous silicon, laser-induced crystallization, transient conductance measurements

### §1. Introduction

A technique for fabricating thin-film transistors (TFT's) is useful in fabricating devices such as liquid crystal displays (LCD) addressed by active matrices. Hydrogenated amorphous silicon (a-Si:H) TFT's<sup>1-4)</sup> have been widely used because they can be fabricated at a low processing temperature of 200-300°C on a glass substrate. A-Si:H TFT's, however, have a channel mobility lower than 1 cm<sup>2</sup>/V·s. So they cannot be applied to devices operating at a high frequency ( $\geq 10$  MHz), such as shift registers.

We have reported the fabrication of polycrystalline silicon (poly-Si) TFT's with a high carrier mobility using XeCl excimer laser crystallization of a-Si:H<sup>5)</sup> at a processing temperature as low as that of conventional a-Si:H TFT's.

In this paper, multistep irradiation of laser pulses is proposed in order to crystallize an a-Si:H film. Moreover, we demonstrate fabrication of poly-Si TFT's at low processing temperatures of 150 and 250°C and discuss the electrical characteristics of these devices.

### §2. Characterization of Laser-Induced Crystallization of a-Si:H Film

In order to determine the optimum condition for crystallization, we investigated the laser-induced melting of a-Si:H film using transient conductance measurements.<sup>6,7)</sup> Figure 1 shows a schematic diagram of the experimental system. A 30 nm-thick a-Si:H film was deposited on a glass substrate at 250°C by decomposition of SiH<sub>4</sub> using radio-frequency glow discharge (rf-GD) and was patterned into 1 mm-wide stripes. Al electrodes with a gap and width of 3 mm were formed on the a-Si:H stripes. The Al electrodes were connected to a load resistor of 50  $\Omega$  and a bias voltage of 10 V was applied. The sample was irradiated with 30 ns-FWHM pulses of an XeCl excimer laser. The laser beam was formed into a 5 mm  $\times$  10 mm rectangle through a lens at the sample surface in order to provide uniform irradiation. The incident energy density was varied by density filters. The transient current during laser treatment was measured across

the load resistor by a high-speed storage oscilloscope. The melting threshold energy was determined by time-resolved optical reflectivity measurements<sup>8)</sup> using an Ar-514.5 nm laser beam as a probe light. The Ar-laser beam was focused by a lens on the center of the sample with a beam diameter of 0.2 mm. The increase of reflectivity associated with the transformation from a solid to a molten state was detected by a high-speed photodiode.

Figure 2 shows the transient conductance caused by the irradiation with a single pulse at an energy density of 240 mJ/cm<sup>2</sup>, which was much larger than the melting threshold energy of 130 mJ/cm<sup>2</sup>. The film melted by irradiation exhibited the large conductance associated with molten silicon for 130 ns before solidifying. The solidified surface became increasingly rough. The roughness was 100-200 nm. The surface roughness was probably caused by hydrogen atoms, which were 10 atomic percent of the as-deposited a-Si:H film, explosively evaporating during the melting caused by single-pulse irradiation at 240 mJ/cm<sup>2</sup>.

In order to prevent the explosive evaporation of hydrogen atoms during crystallization, multistep irradiation

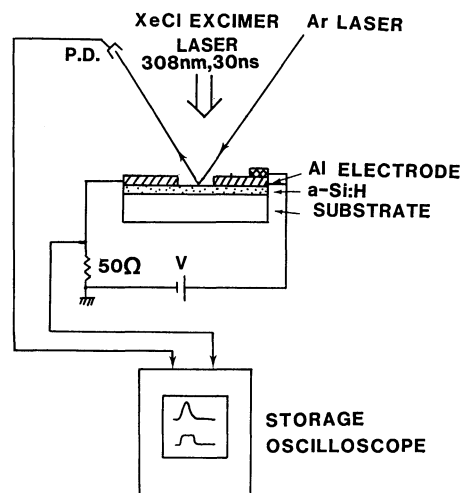


Fig. 1. Schematic diagram of sample and measurement apparatus for transient conductance and time-resolved optical reflectivity.

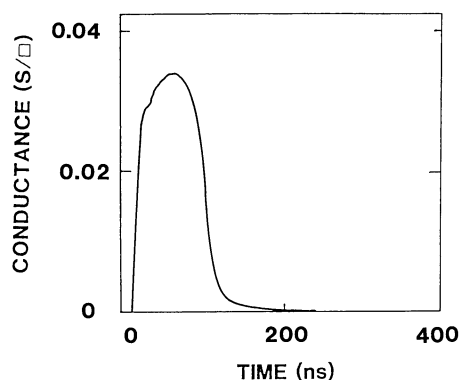


Fig. 2. Conductance vs time for 30 nm-thick a-Si:H film irradiated with a single pulse at 240 mJ/cm<sup>2</sup>.

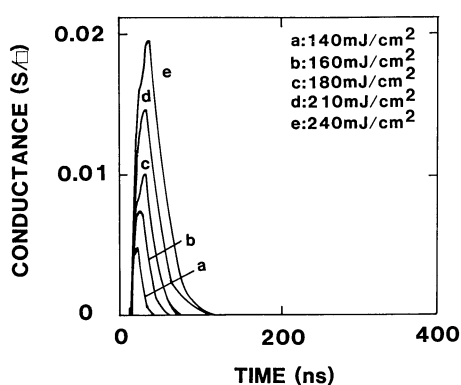


Fig. 3. Evolution of transient conductance with increasing laser energy density for 30 nm-thick a-Si:H film.

tion was carried out. Figure 3 shows the evolution of transient conductance when the energy density was increased from 140 to 240 mJ/cm<sup>2</sup>. The similarity in shape of the conductance curves indicates that the melt and regrowth occurred in the same way at energy densities from 140 to 240 mJ/cm<sup>2</sup> and that the melt depth increased with increasing energy density. In the multistep irradiation, the melt-regrowth with an explosive evaporation of hydrogen, seen in Fig. 2, did not occur. Transmission electron micrograph (TEM) measurements revealed that the a-Si:H film was crystallized completely by the multistep irradiation. Moreover, the surface was very smooth and the roughness was less than 4 nm, which is in contrast to the surface obtained by a single-pulse irradiation at 240 mJ/cm<sup>2</sup>. The grain size is distributed between 10 and 60 nm, as is shown in the bright-field TEM photograph of Fig. 4. The small grains resulted from the short regrowth time of, at most, 100 ns, as can be seen in Fig. 3. The grains had random orientation and a round shape. The dendritic grain growth often observed in solid phase crystallization<sup>9)</sup> did not occur. The results in Fig. 3 and Fig. 4 indicate that the crystallization occurred through random nucleation and rapid solidification of molten silicon.

Hydrogen concentration in the film was measured by Fourier transform spectroscopy (FTIR). Figure 5 shows infrared transmittance spectra of an as-deposited a-Si:H film and a poly-Si film fabricated by multistep irradiation.

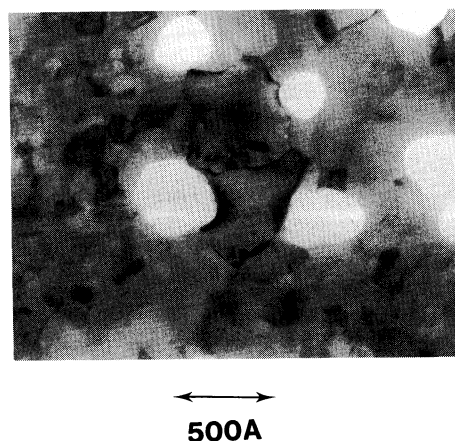


Fig. 4. Bright-field TEM photograph of the poly-Si film fabricated by XeCl excimer-laser-induced crystallization.

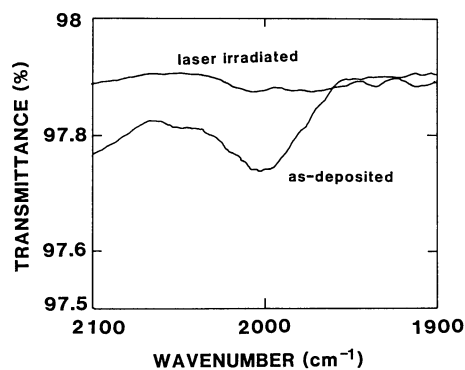


Fig. 5. IR transmittance spectra of an as-deposited a-Si:H film and laser-crystallized film. The thickness of the films was 30 nm.

The a-Si:H film has a hydrogen concentration of about 10 atomic percent, and the IR spectrum had the broad curve around 2000 cm<sup>-1</sup> associated with absorption of the stretching vibration mode between a silicon and a hydrogen atom (Si-H). After crystallization, the Si-H absorption intensity was below the noise level. The hydrogen concentration, therefore, was lower than 0.2 atomic percent after the laser-induced crystallization process.

### §3. Fabrication and Characterization of Poly-Si TFT's

Poly-Si TFT's with the structure shown in Fig. 6 were fabricated. In this process, TFT's were fabricated at processing temperatures of 150°C and 250°C, corresponding to the temperatures of rf-GD deposition of 20 nm-thick a-Si:H and SiO<sub>2</sub> films. The a-Si:H film was crystallized at

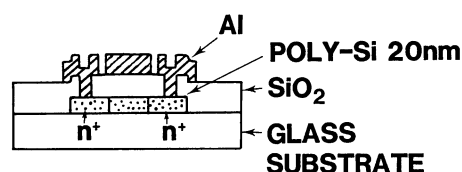


Fig. 6. Schematic cross section of the poly-Si TFT fabricated using XeCl excimer laser annealing process.

room temperature by multistep irradiation with 10 laser pulses at a maximum energy density of  $240 \text{ mJ/cm}^2$ . At each step of irradiation, the amount of laser energy being small, the substrate was heated no more than  $180^\circ\text{C}$  at a point  $600 \text{ nm}$  under the top silicon layer.\* Source and drain regions were formed simultaneously when a-Si:H was crystallized. The channel region was coated with photoresist for protection against doping. A  $5 \text{ nm}$ -thick phosphorus-doped a-Si:H (a-Si:H, P) film for the dopant source was subsequently deposited at  $100^\circ\text{C}$  by decomposition of a gas mixture with  $20 \text{ SCCM SiH}_4$  and  $1 \text{ SCCM PH}_3$  using rf-GD. The photoresist and a-Si:H, P on the photoresist were then removed. The laser-induced melting diffused phosphorus atoms into the film, and regions with a low sheet resistance of  $600 \Omega/\square$  were formed. Figure 7 shows the dependence of resistivity of a phosphorus-doped poly-Si film on laser energy density. The laser-induced melting decreased resistivity from  $5 \times 10^4 \Omega \cdot \text{cm}$  of the as-deposited a-Si:H film to  $5 \times 10^{-4} \Omega \cdot \text{cm}$  because the crystallization of a-Si:H and a-Si:H, P caused an increase in carrier mobility and an increase in the activation of phosphorus atoms.<sup>10,11)</sup> After the irradiation, poly-Si islands were formed. An  $\text{SiO}_2$  layer was subsequently deposited by decomposition of mixture gases with  $2 \text{ SCCM SiH}_4$  and  $100 \text{ SCCM N}_2\text{O}$  for the gate insulator. Contact holes were opened at source and drain regions, and an Al layer was deposited to pattern the gate, source and drain electrodes. The sample was finally annealed in hydrogen plasma at  $150^\circ\text{C}$  for 30 minutes at an rf-power of  $5 \text{ W}$  in order to terminate dangling bonds at the grain boundaries in poly-Si film. Figures 8(a) and 8(b) show drain-current-vs-drain-voltage ( $I_D - V_D$ ) characteristics and drain-current-vs-gate-voltage ( $I_D - V_G$ ) characteristics, respectively, for a poly-Si TFT with a  $300 \text{ nm}$ -thick gate- $\text{SiO}_2$  layer fabricated at  $150^\circ\text{C}$ . The on/off current ratio at a drain voltage of  $5 \text{ V}$  between gate voltages of  $-10 \text{ V}$  and  $20 \text{ V}$  is  $2 \times 10^6$ . The effective carrier mobility in the linear region is  $24 \text{ cm}^2/\text{V} \cdot \text{s}$ , which is much larger than that of conventional a-Si:H TFT's. This result indicates that poly-Si TFT's with a high

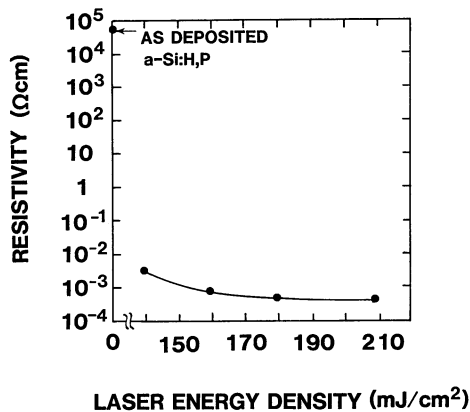


Fig. 7. Dependence of conductivity on laser energy density during crystallization of a-Si:H, P film.

\*T. Sameshima, H. Tomita, M. Hara and S. Usui: Extended Abstracts (the 36th Spring Meeting, 1989) The Japan Society of Applied Physics and Related Societies, 1p-PC-40.

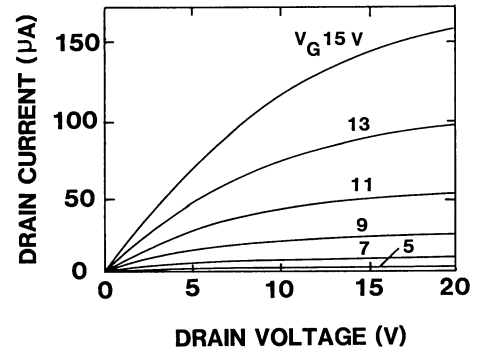


Fig. 8. (a) Drain-current-vs-drain-voltage characteristics of the poly-Si TFT fabricated at  $150^\circ\text{C}$ . Gate width and gate length are  $300 \mu\text{m}$  and  $30 \mu\text{m}$ , respectively.

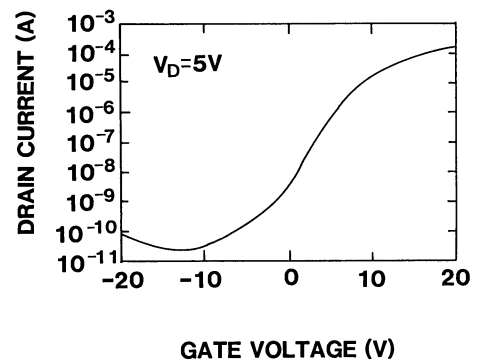


Fig. 8. (b) Drain-current-vs-gate-voltage-characteristics of the poly-Si TFT fabricated at  $150^\circ\text{C}$ . Gate width and gate length are  $300 \mu\text{m}$  and  $30 \mu\text{m}$ , respectively.

mobility can be fabricated using XeCl excimer laser annealing at a very low processing temperature.  $I_D - V_G$  characteristics, however, had a low subthreshold slope of  $1.5 \text{ V/decade}$ . This indicates that the electric characteristics of the interface between  $\text{SiO}_2$  and poly-Si were not ideal because of the large trapping-state density.

The  $I - V$  characteristics of the poly-Si TFT's were improved when the higher processing temperature was used. Figures 9(a) and 9(b) show  $I_D - V_D$  characteristics and  $I_D - V_G$  characteristics, respectively, for a poly-Si TFT with a  $100 \text{ nm}$ -thick gate  $\text{SiO}_2$  layer fabricated at  $250^\circ\text{C}$ . The on/off current ratio at a drain voltage of  $5 \text{ V}$  between gate voltages of  $-5 \text{ V}$  and  $20 \text{ V}$  is  $1.5 \times 10^7$ . The effective carrier mobility in the linear region was  $54 \text{ cm}^2/\text{V} \cdot \text{s}$ . The minimum subthreshold slope was  $0.38 \text{ V/decade}$ . These results show that trapping-state density and potential barrier height at the grain boundaries are small for poly-Si TFT fabricated at  $250^\circ\text{C}$ . When the current is governed by thermionic emission around grain boundaries in poly-Si, the drain current in the linear region is given by<sup>12,13)</sup>

$$I_D = (W/L) \cdot V_D \cdot C_{ox} \cdot V_G \cdot \mu_o \cdot \exp(-E_B/kT), \quad (1)$$

where  $W/L$  is the geometrical factor,  $C_{ox}$  is the oxide capacitance per unit area,  $\mu_o$  is the preexponential factor,  $k$  is the Boltzman constant, and  $T$  is the absolute temperature.  $E_B$  is the potential barrier height given by<sup>12,13)</sup>

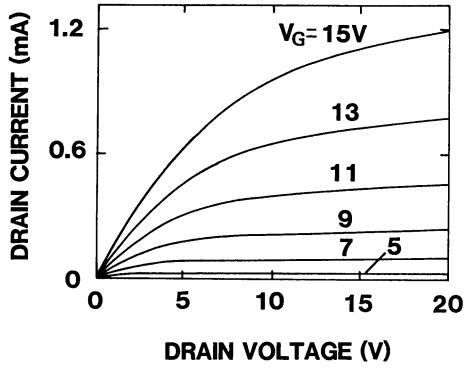


Fig. 9. (a) Drain-current-vs-drain-voltage characteristics of the poly-Si TFT fabricated at 250°C. Gate width and gate length are 300  $\mu\text{m}$  and 30  $\mu\text{m}$ , respectively.

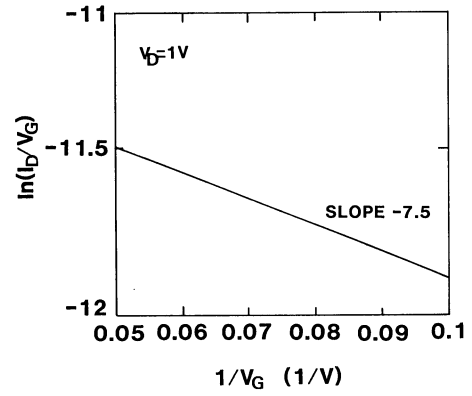


Fig. 10.  $\ln(I_D/V_G)$  vs  $(1/V_G)$  for the poly-Si TFT fabricated at 250°C.

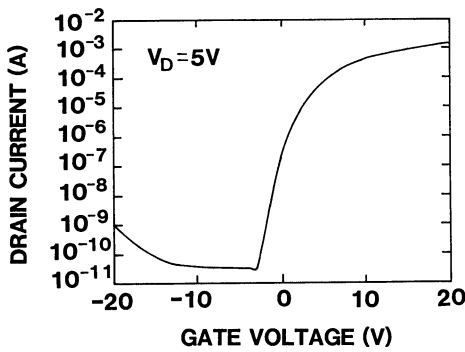


Fig. 9. (b) Drain-current-vs-gate-voltage characteristics of the poly-Si TFT fabricated at 250°C. Gate width and gate length are 300  $\mu\text{m}$  and 30  $\mu\text{m}$ , respectively.

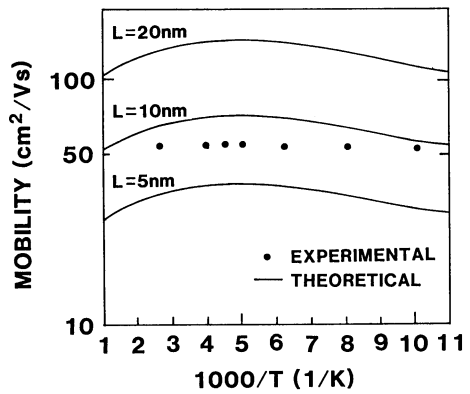


Fig. 11. Dependence of experimental and theoretical mobility on temperature.

$$E_B = q^3 \cdot N_t^2 \cdot d / (8 \cdot \epsilon_s \cdot C_{ox} \cdot V), \quad (2)$$

where  $q$  is the electric charge,  $N_t$  is the carrier trap-state density per unit area,  $\epsilon_s$  is the semiconductor permittivity, and  $d$  is the depth of the channel region of 20 nm, which was obtained by Stern's calculation for a MOS structure at 300 K.<sup>14</sup> Equations (1) and (2) give  $N_t$  as the slope of  $\ln(I_D/V_G)$ -vs- $(1/V_G)$ . Figure 10 shows the  $\ln(I_D/V_G)$ -vs- $(1/V_G)$  characteristics of the poly-Si TFT fabricated at 250°C. The potential barrier height was 0.01 eV at  $V_G$  of 20 V and the carrier trap-state density was  $1.0 \times 10^{12} \text{ cm}^{-2}$ . The value of the potential barrier height was lower than that of conventional poly-Si TFT's.<sup>13</sup> The low potential barrier height resulted in the high carrier mobility of the poly-Si film fabricated by XeCl-excimer-laser-induced crystallization of a-Si:H although the grain size was small, as can be seen in Fig. 4.

The carrier mobility in poly-Si was given by<sup>15)</sup>

$$\mu = L \cdot q \cdot (2\pi mkT)^{-0.5} \exp(-E_B/kT), \quad (3)$$

where  $L$  is the average grain size and  $m$  is the effective mass of electron. Figure 11 shows dependence of the effective carrier mobility of the poly-Si TFT on the temperature between 145 K to 350 K and the calculated mobility with  $E_B$  of 0.01 eV using eq. (3). The mobility of the poly-Si TFT does not change with temperature. The

calculated mobility did not depend greatly on temperature, either. The experimental mobility of the poly-Si TFT is close to the calculated mobility if the grain size is assumed to be 10 nm, the size of the smallest grain in Fig. 11. This shows that the mobility is determined by carrier transfer in the region with the smallest grains seen in the photograph of Fig. 4.

#### §4. Conclusions

Polycrystalline silicon film with a smooth surface was fabricated by laser-induced melting of a glow-discharge-produced a-Si:H film with multistep irradiation of XeCl excimer laser pulses. The grain size was distributed between 10 and 60 nm. Hydrogen concentration in the crystallized film was lower than 0.2 atomic percent.

A poly-Si TFT fabricated at 250°C had a large carrier mobility of  $54 \text{ cm}^2/\text{V}\cdot\text{s}$ . The on/off current ratio was  $1.5 \times 10^7$ . The potential barrier height at the grain boundaries was 0.01 eV, indicating that the poly-Si film fabricated by laser-induced melt and regrowth had good electric properties. A poly-Si TFT was also fabricated at 150°C. Its carrier mobility was  $24 \text{ cm}^2/\text{V}\cdot\text{s}$ , which is much larger than that of conventional a-Si:H TFT's.

These results show that poly-Si TFT's with a high mobility can be fabricated using excimer laser-induced crystallization at processing temperatures lower than that

of the conventional a-Si:H TFT fabrication process.

### Acknowledgements

The authors would like to thank M. Nakagoe and K. Kunisada for their experimental support and Dr. Y. Kawana for the helpful discussions. They also wish to acknowledge the support of Dr. M. Kikuchi.

### References

- 1) Y. Ugai, Y. Murakami, J. Tamamura and S. Aoki: *1984 SID Int. Symp. Digest of Technical Papers, San Francisco* (Society for Information Display, New York, NY, 1984) p. 308.
- 2) F. Fukuda, Y. Takafuji, K. Yano, H. Take and M. Matsuura: *1986 SID Int. Symp. Digest of Technical Papers, San Diego* (Society for Information Display, New York, NY, 1986) p. 293.
- 3) S. Hotta, S. Nagata, Y. Miyata and K. Yokoyama: *1986 SID Int. Symp. Digest of Technical Papers, San Diego* (Society for Information Display, New York, NY, 1986) p. 298.
- 4) V. Lebosq, M. LeContellec, F. Morin, S. Slaun and F. Weisse: *Proc. on 1985 International Display Research Conference, San Diego* (Institute of Electrical and Electronics Engineers, New York, NY, 1985) p. 34.
- 5) T. Sameshima and S. Usui: *Proc. MRS(1986) on Material Issues in Silicon Integrated Circuit Proceedings*, eds. M. Wittmer, J. Stinmel and M. Strathmann (Material Research Society, Pittsburgh, PA, 1986) p. 435.
- 6) Gavlin, M. O. Thompson, J. N. Mayer, R. B. Hammond, N. Paulter and P. S. Peercy: *Phys. Rev. Lett.* **48** (1982) 33.
- 7) T. Sameshima, H. Tomita and S. Usui: *Jpn. J. Appl. Phys.* **27** (1988) L1935.
- 8) D. H. Auston, J. A. Golovchenko, P. R. Smith, C. M. Surko and T. N. C. Venkatesan: *Appl. Phys. Lett.* **33** (1978) 538.
- 9) R. B. Iverson and R. Reif: *J. Appl. Phys.* **57** (1985) 5169.
- 10) T. Sameshima, S. Usui: *Proc. MRS (1986) on Laser and Particle Beam Chemical Processing for Microelectronics*, eds., D. J. Ehrlich, G. S. Higashi and M. M. Oprysko (Material Research Society, Pittsburgh, PA, 1987) p. 491.
- 11) T. Sameshima, S. Usui and H. Tomita: *Jpn. J. Appl. Phys.* **26** (1987) L1678.
- 12) J. Levinson, F. R. Sheherd, P. J. Scanlon, W. D. Westwood, G. Este and M. Rider: *J. Appl. Phys.* **53** (1982) 1193.
- 13) T. Takeshita, T. Unagami and O. Kogure: *Jpn. J. Appl. Phys.* **27** (1988) 1937.
- 14) F. Stern: *Phys. Rev.* **B5** (1972) 4891.
- 15) J. Y. W. Seto: *J. Appl. Phys.* **48** (1975) 5297.